Surface alloys as interfacial layers between quasicrystalline and periodic materials

2008 J. Phys.: Condens. Matter 20 314009

(http://iopscience.iop.org/0953-8984/20/31/314009)

J. Phys.: Condens. Matter **20** (2008) 314009 (8pp) doi:10.1088/0953-8984/20/31/314009

Surface alloys as interfacial layers between quasicrystalline and periodic materials

T Duguet, J Ledieu, J M Dubois and V Fournée[1]

Laboratoire de Science et Génie des Matériaux et de Métallurgie, UMR 7584 CNRS-Nancy Université, Ecole des Mines de Nancy, Parc de Saurupt, F-54042 Nancy, France

E-mail: fournee@lsg2m.org

Received 28 April 2008
Published 11 July 2008
Online at stacks.iop.org/JPhysCM/20/314009

Abstract

Low adhesion with normal metals is an intrinsic property of many quasicrystalline surfaces. Although this property could be useful to develop low friction or non-stick coatings, it is also responsible for the poor adhesion of quasicrystalline coatings on metal substrates. Here we investigate the possibility of using complex metallic surface alloys as interface layers to enhance the adhesion between quasicrystals and simple metal substrates. We first review some examples where such complex phases are formed as an overlayer. Then we study the formation of such surface alloys in a controlled way by annealing a thin film deposited on a quasicrystalline substrate. We demonstrate that a coherent buffer layer consisting of the γ-Al_4Cu_9 approximant can be grown between pure Al and the *i*-Al–Cu–Fe quasicrystal. The interfacial relationships between the different layers are defined by $[111]_{Al} \parallel [110]_{Al_4Cu_9} \parallel [5f]_{i\text{-Al–Cu–Fe}}$.

(Some figures in this article are in colour only in the electronic version)

1. Introduction

Adherence of quasicrystalline coatings on a metallic substrate is usually poor and this is problematic regarding potential applications of these materials. This poor adherence is intrinsic to quasicrystalline surfaces [1, 2]. Indeed, adhesion forces between metals and quasicrystals (QCs) are significantly lower than for a metal-on-metal contact. This has been verified at different length scales and under different conditions, from ultra-high vacuum (UHV) conditions up to atmospheric pressure [2]. Low adhesion, like other surface properties of quasicrystals, has been correlated with the aperiodic long-range order and the associated complex electronic structure [3–5]. Whereas this low adhesion property can clearly be useful when used as a coating for non-sticking or low friction applications, the same property will be detrimental to the adherence of the coating on the substrate.

A way to circumvent this problem is to tailor the adherence of the QC coating by growing an interface layer between substrate and coating. The interface layer should present intermediate properties between the metal substrate and the QC. It should also have the ability to promote an epitaxial relationship with both the metal substrate and the QC. Such phases potentially exist in neighbouring regions of the phase diagram and are called approximant crystals. Approximants are intrinsically related to their parent QC. More precisely, in the framework of the cut method, the structure of a QC and its approximants can be derived from the same periodic object in a hyperspace of dimension $N > 3$. Depending on the relative orientation of the three-dimensional (3D) physical subspace embedded in the hyperspace, the same N-dimensional periodic object will lead to either a quasiperiodic structure or a periodic approximant, via the cut and projection method [6]. High-order approximants have giant unit cells containing several hundreds of atoms arranged into highly symmetric clusters similar to those found in QC structures. This definition of an approximant has been extended to other structurally simpler phases, usually superstructures based on vacancy-ordered CsCl units [7]. These latter phases are termed 'approximant' in the sense that they locally exhibit distorted fivefold atomic configurations along certain crystallographic directions and have similar valence electron concentrations as the corresponding QC phase. The properties of various approximants have been investigated in comparison to quasicrystals and it follows that the physical behaviour of these phases gradually evolves towards the anti-metallic character typical of QCs with increasing structural complexity [8]. Therefore, *a priori*, approximant phases fulfil

[1] Author to whom any correspondence should be addressed.

both requirements listed above in order to be used as an interfacial layer between a QC coating and a metallic substrate.

In this paper, we investigate the possibility of growing such an interface buffer layer. In section 2, we review the different studies reporting the formation of approximant phases on top of a QC substrate resulting from preferential evaporation or sputtering of some component of the ternary alloy. Then in section 3 we will describe situations where intermixing between adsorbate elements and the QC substrate leads to the formation of a surface alloy. The following section 4 will describe new experimental results on the growth of Cu thin films on the fivefold surface of the icosahedral (*i*-) Al–Cu–Fe quasicrystal. For coverages ranging from 2–7 monolayers (ML), Cu intermixes with the substrate readily at room temperature, resulting in the formation of a surface alloy identified as the β-Al(Cu, Fe) bcc phase. Upon further deposition, a bulk-like Cu thin film grows on top of the β buffer layer. Furthermore, by annealing a 20 ML thick Cu film, we promote the formation of another approximant phase identified as the γ-Al_4Cu_9 phase. Finally, this surface alloy is used as an interface layer in a stacking sequence of Al(111)/Al_4Cu_9(110)/*i*-Al–Cu–Fe (fivefold, or 5f).

2. Phase transformations on quasicrystalline surfaces

Most QCs are obtained from a ternary melt containing a large amount of Al, typically 60–70 at.%, alloyed with transition metals, most often 3d and 4d elements. The stabilization of such a complex structure is attributed to a combination of both Hume-Rothery and sp–d hybridization effects, leading to the formation of a minimum in the density of states located in the vicinity of the Fermi level (E_F) [9]. This so-called pseudogap is a consequence of the interaction between the Fermi sphere and the pseudo-Jones zone, constructed from the Bragg planes corresponding to intense diffraction peaks. The Bragg scattering of the electronic waves is further enhanced by a hybridization mechanism. The induced depletion of electronic states at E_F contributes to the stabilization of the QC phase by lowering the total free energy. The formation of the pseudogap goes along with a specific ratio of valence electrons per atom that determines the radius of the Fermi sphere. This explains in part the observation that QC usually form in a narrow composition range. When deviating from this small concentration domain, QCs decompose into neighbouring phases of the phase diagram, which are generally approximants [10] or B2, CsCl-type β phases. Such phase transformations at the solid state have been observed many times in surface studies of various quasicrystalline systems.

Surface science requires the use of large single-grain QCs which must be cleaned in ultra-high vacuum (UHV) for investigation. Two different types of surface preparation are typically used; either fracture in UHV to expose a fresh surface or cycles of ion sputtering followed by annealing treatments. The former leads to a rough surface morphology [11] and is sample-consuming. Therefore the latter method is the most commonly used and it has the advantage of producing a step–terrace morphology [12], suitable for scanning tunnelling microscopy (STM) experiments, for example. However, when sputtering the surface of a QC, one or more elements are preferentially removed from the surface and a proper annealing is needed to recover the composition and structure of the bulk. This general trend has been reported in several papers. Table 1 summarizes the evolution of the near-surface chemical composition and atomic structure during the sputter–annealing cycle for several high-symmetry surfaces of *i*-Al–Cu–Fe and *i*-Al–Pd–Mn QCs [13–16]. In both systems, a drastic Al depletion is observed, giving rise to the formation of β phases with CsCl structure type, in accordance with the phase diagram. In the case of the Al–Cu–Fe system, the lattice parameter of the β-Al(Cu, Fe) is $a = 2.909$ Å and the space group is $Pm3m$. Al atoms occupy the corner sites and Fe and Cu occupy randomly the body centred sites of the unit cell. The β phase appears either directly after sputtering or after low-temperature annealing. Except for the threefold surface of *i*-Al–Pd–Mn, the interface plane between the β overlayer and the QC is defined by the $[110]_\beta$ direction being parallel to either the fivefold or twofold axis of the substrate [13–16]. The symmetry of the substrate, however, affects the number of possible in-plane orientations. For the twofold surface, β-(110) domains exist in two different orientations, whereas five different domains coexist on the fivefold surface, rotated by 72°. The structure of the sputter-induced overlayer is usually derived from a low-energy electron diffraction (LEED) pattern or reflection high-energy electron diffraction (RHEED). A more detailed surface structure determination was performed by Shi *et al* [14] on a sputtered fivefold *i*-Al–Cu–Fe surface annealed at temperatures ranging from 550 to 650 K for 2 h. Using dynamical low-energy electron diffraction (LEED $I(V)$), a best fit was found using a surface model consisting of unreconstructed β-Al(Cu, Fe) with (110) orientation, with Al atoms buckling out of the surface by 0.18 Å, due to the relative size and electronegativity of Al compared to the other elements.

Other CsCl-based structures were reported on *i*-Al–Pd–Mn and *i*-Al–Cu–Fe QC surfaces by Shen and coworkers [13] and a simple explanation for the frequent occurrence of such B2 phases on QC surfaces was proposed, based on the fact that only small displacements of atoms are needed to transform a bcc packing into an icosahedral packing.

For higher annealing temperature, the chemical composition and the quasiperiodic structure are restored. The required temperature is obviously system-dependent. As an alternative to diffraction experiments, it is possible to follow the QC surface recovery by observing the formation of the pseudogap upon annealing. Figure 1 shows ultraviolet photoemission spectra (UPS) recorded on the fivefold *i*-Al–Cu–Fe surface after sputtering and after different annealing temperatures [15]. By fitting the Fermi edge, the authors could show that a pseudogap developed progressively with increasing annealing temperature, illustrating the transition from a metallic-like system to a quasicrystal. Similar observations were made by UPS on the twofold surface of *i*-Al–Pd–Mn after sputtering and annealing up to 973 K [16].

Although only simple CsCl-based structures have been observed so far as overlayers on the Al–Cu–Fe system, the formation of more complex alloys has been reported on the Al–Pd–Mn surface upon sputtering–annealing. A stable decagonal

Table 1. Chemical composition and structure of various QC surfaces measured after sputtering and annealing at different temperatures. Details on the preparation and experiments can be found in [13–16].

		Auger electron spectroscopy				
	Annealing T (K)	Al (%)	Pd (%)	Mn (%)	LEED	
2f-Al–Pd–Mn	300	61	33	6	No pattern	Shen *et al*
	600	68	27	5	Two bcc (110) domains	
	900	73	19	7	Twofold i-QC	
3f-Al–Pd–Mn	300	49	45	5	3 facets	
	600	62	36	2	3 facets + cubic (111)	
	800	74	20	6	Threefold i-QC	
5f-Al–Pd–Mn	300	52	43	5	No pattern	
	600	63	33	4	Five bcc (110) domains	
	850	71	23	6	Fivefold i-QC	
		X-ray photoelectron spectroscopy			LEED/XPD	
5f-Al–Pd–Mn	300	53	41	6	5 bcc domains	Naumovic *et al*
	823	68	26	6	Fivefold i-QC	
	923	76	11	13	Tenfold d-QC	
2f-Al–Pd–Mn	300	54	42	4		
	638	61	37	2	2 bcc (110) domains	
	683	70	26	4	rotated by 109°	
	823	73	22	5		
	973	68	27	5	Twofold i-QC	
		Auger electron spectroscopy				
		Al (%)	Cu (%)	Fe (%)	LEED	
5f-Al–Cu–Fe	300	54	22	24	No pattern	Shen *et al*
	600	64	18	18	Five bcc (110) domains	
	800	72	18	10	5f-fold i-QC	
5f-Al–Cu–Fe	550–650	64	18	18	Five cubic β-(110)	Shi *et al*
	750	73	16	10	Fivefold i-QC	
		X-ray photoelectron spectroscopy			RHEED	
5f-Al–Cu–Fe	300	50	34	16	Five cubic β-(1-10)	Barrow *et al*
	570	64	22	14	Domains	
	670	62	27	11	β-spots fading	
	770	64	26	10	QC pattern	

(d-) Al–Pd–Mn surface alloy was reported upon annealing the fivefold surface of i-Al–Pd–Mn at 923 K [17]. This phase was attributed to the enrichment of the surface with Mn during annealing at high temperature. The orientation relationship with the isocahedral substrate was determined by x-ray photoelectron diffraction (XPD). The decagonal phase has its tenfold axis parallel to the fivefold axis of the i-Al–Pd–Mn substrate. Ledieu and coworkers also observed the occurrence of an orthorhombic approximant phase T-Al_3Mn after annealing above 970 K [18]. The measured composition was $Al_{75}Pd_6Mn_{19}$, i.e. very close to Al_3Mn. The same kind of T-phase formation on the fivefold surface of i-Al–Pd–Mn was reported after annealing at 920 K [19].

Another complex phase was observed after annealing the same sample at lower temperature (770 K) [19]. The structure of this phase was characterized by STM (figure 2). The lattice parameters of the rectangular unit cell of this surface alloy derived from these images are found equal to $a = 1.9$ Å and $b = 4.8$ Å. This does not correspond to any known bulk phase.

These results illustrate the great variety of complex surface phases which can be formed on QCs, with good orientational epitaxy. However, in these experiments, these alloys were formed by 'accident' during QC surface preparation. No control over the chemical composition can be achieved during the sputter–annealing process and thus this method does not appear to be valid for the formation of well-defined interface buffer layers. Therefore, we will focus in the next section on the formation of surface alloys induced by controlled interdiffusion of an adsorbate with substrate atoms.

3. Surface alloys grown on quasicrystalline surfaces

Studies of surface alloys induced by deposition of a metal A on a substrate B is a subject in itself (see, e.g., [20]). In most studies, substrate B is a simple metal and alloying occurs either at room temperature or must be activated by annealing. Here we are facing an additional degree of complexity because the metal adsorption occurs on a ternary alloy. However, the surface of Al-rich QCs like i-Al–Pd–Mn or i-Al–Cu–Fe corresponds to a bulk truncation consisting of an Al-rich top layer followed by a plane containing transition metals and located just 0.42 Å below [21–24]. The density of this surface

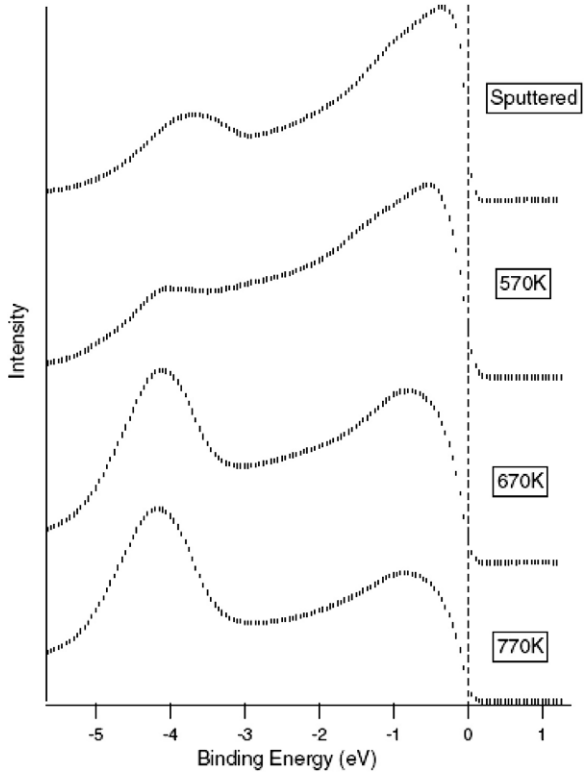

Figure 1. Room temperature photoemission valence band spectra of the fivefold *i*-Al–Cu–Fe surface, measured using He I (21.2 eV) radiation for different annealing temperatures. Sputtering conditions were (Ar^+, 5 keV). Reprinted with permission from [15]. Copyright 2003, Elsevier.

termination is similar to that of an Al(111) surface. Therefore it may be useful to compare the deposition of a metal on a QC with the binary metal-on-Al system. We reproduce in table 2 a summary of experimental data on intermixing in an Al–transition metal (TM) bilayered system, taken from Buchanan *et al* [25]. Intermixing lengths reported in this table were obtained using grazing incidence x-ray reflectivity on samples of TM on Al and Al on TM deposited by magnetron sputtering (200 W, 350 V, $p_{Ar} = 0.27$ Pa) at room temperature. As can be seen from table 2, the degree of intermixing at room temperature is surprisingly large in many Al–TM systems. This is especially true for Co–Al, Cu–Al and Au–Al bilayers [25].

In the following, we provide some examples showing that such a comparison between TM–Al bilayers and TM on Al-rich QCs is relevant. Shimoda *et al* studied the growth of an Au thin film deposited on the tenfold *d*-Al–Ni–Co or the fivefold *i*-Al–Pd–Mn surfaces [26, 27]. At submonolayer coverage, the formation of twinned CaF_2-type $Al_2Au(110)$ domains was observed at room temperature. For higher coverage (≈10 ML), the same surface alloy is formed on *d*-Al–Ni–Co or *i*-Al–Pd–Mn: however, the use of In as a surfactant and a soft annealing (350–400 K) was necessary. Therefore, as expected from the intermixing length of bilayers at room temperature, Al–Au compounds can be formed on the QC substrate. Another example is the adsorption of Co on *i*-Al–Pd–Mn reported by Weisskopf *et al* [28]. At low coverage, it was found that Co deposition leads to the continuous formation of a CsCl-type

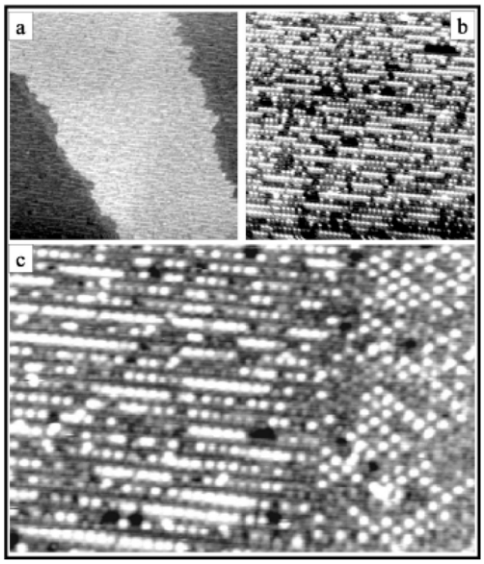

Figure 2. STM images obtained after decomposition of the fivefold *i*-Al–Pd–Mn surface at 770 K. Reprinted with permission from [19]. Copyright 2002 by the American Physical Society.

AlCo(110) surface alloy already at room temperature. Five domains rotated by 72° from each other are responsible for the observed pseudo-tenfold LEED pattern. For larger coverages (above 2 ML), Co grows epitaxially on the interfacial layer of AlCo, adopting the bcc (110) structure. This last example illustrates the relevance of the use of intermixing data (table 2) to predict general trends for metals on QCs. It also shows the potential use of surface alloys as interfacial layers between QCs and metallic layers.

Finally, Bielmann *et al* showed that γ-Al_4Cu_9 is formed by deposition of Cu on a monocrystalline *i*-Al–Pd–Mn QC sample and subsequent annealing (623 K) [29]. The γ-Al_4Cu_9 phase is interesting as it has been described as an approximant of the *i*-Al–Cu–Fe QC [30] which exhibits a surprisingly low friction coefficient against hard steel in vacuum [4]. Its surface energy is estimated to be close to that of aluminium (typically 1 J m^{-2}) [4]. It is a cubic phase based on a 3 × 3 × 3 superstructure of CsCl unit cells containing two vacancies. Unlike many simple CsCl-type structures presented above, it exhibits a valence electron concentration similar to that of the *i*-Al–Cu–Fe phase, and pentagonal configurations within its (110) plane. Those elements make it a good candidate for potential use as an interfacial layer between a QC coating and a metallic substrate in order to get a good orientation relationship and good adherence. In the next section, we present new experimental results describing the formation of this phase on the fivefold surface of the *i*-Al–Cu–Fe substrate.

4. The γ-Al_4Cu_9 surface alloy as an interface buffer layer

4.1. Experimental details

The following experiments were performed in a UHV multi-chamber system with a base pressure of ∼5 × 10^{-11} mbar. A clean fivefold *i*-Al–Cu–Fe surface was prepared by sputtering (Ar^+, 2 keV) and annealing (913 K) cycles. The quasiperiodic

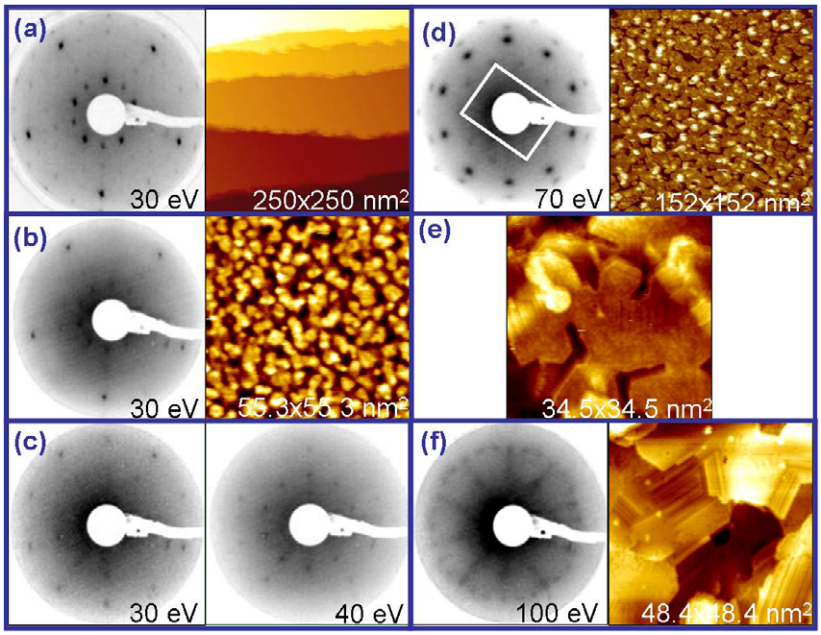

Figure 3. LEED pattern and STM image of the clean surface (a) and after dosing 0.5 ML on *i*-Al–Cu–Fe (b). (c) shows two LEED patterns obtained after 1 ML deposition. (d) shows typical LEED and STM images for a coverage ranging from 2 to 8 ML. (e) Typical LEED pattern and STM image obtained for a 20 ML thick Cu film on *i*-Al–Cu–Fe.

Table 2. Intermixing lengths, in Å, for transition metals grown on Al and Al grown on transition metals. Bilayers are systematically formed at room temperature by magnetron sputtering (200 W, 350 V, $p_{Ar} = 0.27$ Pa). Reprinted with permission from [25]. Copyright 2002 by the American Physical Society.

Ti		V		Cr		Mn		Fe		Co		Ni		Cu	
Al	Ti	Al	V	Al	Cr	Al	Mn	Al	Fe	Al	Co	Al	Ni	Al	Cu
On	On	On	On	On	On	On	On	On	On	On	On	On	On	On	On
Ti	Al	V	Al	Cr	Al	Mn	Al	Fe	Al	Co	Al	Ni	Al	Cu	Al
17	50	26	94	5	33	104	151	9	21	8	68	14	79	28	168
Zr		**Nb**		**Mo**		**Tc**		**Ru**		**Rh**		**Pd**		**Ag**	
Al	Zr	Al	Nb	Al	Mo			Al	Ru	Al	Rh	Al	Pd	Al	Ag
On	On	On	On	On	On			On	On	On	On	On	On	On	On
Zr	Al	Nb	Al	Mo	Al			Ru	Al	Rh	Al	Pd	Al	Ag	Al
10	51	8	36	13	34			8	52	4	47	48	56	25	45
Hf		**Ta**		**W**		**Re**		**Os**		**Ir**		**Pt**		**Au**	
Al	Hf	Al	Ta	Al	W	Al	Re	Al	Os	Al	Ir	Al	Pt	Al	Au
On	On	On	On	On	On	On	On	On	On	On	On	On	On	On	On
Hf	Al	Ta	Al	W	Al	Re	Al	Os	Al	Ir	Al	Pt	Al	Au	Al
20	44	1	9	1	35	21	86	1	71	2	54	19	45	52	63

structure of the surface was checked by LEED and STM before each thin film deposition. Copper thin films were grown using an e-beam evaporator whereas Al thin films were grown using a cold-lip effusion cell. Al and Cu purity was 99.999% and the pressure was kept below 2×10^{-10} mbar during deposition. Fluxes were calibrated by analysis of STM images at submonolayer coverage and were determined equal to 0.002 and 0.05 ML s^{-1} for Cu and Al, respectively. The coverage investigated ranged from 0.5 to 20 ML.

The structure of the film was monitored as a function of coverage (θ) and annealing temperature using STM (Omicron VT-STM) and LEED. The lattice parameters deduced from the LEED patterns were obtained by scaling the reciprocal space using a clean Cu(111) sample for each beam energy. The sample was heated by an e^--beam stage, and annealing temperatures mentioned in the following correspond to the temperature measured by the thermocouple attached to the manipulator close to the sample surface. Additional measurements by optical pyrometry (emissivity 0.35) showed that the surface temperature is actually 70 °C above the thermocouple value, within the temperature range investigated (up to 573 K). We will nevertheless refer to the thermocouple temperature in the following as it is not possible to use the optical pyrometer for *in situ* annealing experiments.

4.2. Room temperature growth

The room temperature growth is monitored by LEED and STM for 12 different coverages, from 0 to 20 ML

(0, 0.5, 1, 2, . . . , 8, 12, 20). Figure 3 shows the evolution of the LEED pattern together with STM images for relevant coverages. The clean surface (figure 3(a)) presents large atomically flat terraces separated by steps and the corresponding LEED pattern is consistent with a well-ordered fivefold *i*-Al–Cu–Fe surface. After deposition of 0.5 monolayers (ML) of Cu (figure 3(b)), STM images reveal the formation of small islands with monoatomic heights (2 Å) on the surface. The average island size is estimated from these images at 25 nm^2. At this coverage, the LEED pattern still shows fivefold symmetry but the number of spots is reduced. This is consistent with a previous report on this system by Sharma *et al* [31]. At 1 ML, additional LEED spots appear, suggesting that another phase is developing (see figure 3(c)). Figure 3(d) is representative of the typical LEED patterns and STM images observed for coverages ranging from 2 to 8 ML. The observed pseudo-tenfold pattern consists of five rotational domains, which are rotated by 72° from each other. Distances measured in reciprocal space (rectangular unit cell drawn on the LEED pattern in figure 3(d)) correspond to a unit mesh of 4.10 Å × 2.91 Å in direct space. When comparing to crystallographic data, the dimensions of this surface unit cell are consistent with the (110) orientation of the β-Al(Cu, Fe) phase whose lattice parameter $a = 2.902$–2.908 Å [32]. Figure 3(d) also shows an STM image for 5 ML Cu, indicating a pseudo-layer-by-layer growth. At 8 ML, a more 3D growth is observed with larger faceted domains (figure 3(e)). The measured angles between the facets (∼125°) are expected from the structure of the $(110)_{bcc}$ plane. Finally, from 8 to 20 ML, a new pattern appears consisting of a ring of 30 spots with a diameter corresponding to 2.54 Å in direct space (figure 3(f)). This corresponds to bulk-like Cu growing with five rotational domains with the (111) axis normal to the surface. Atomic rows can be observed on STM images which must be responsible for the stripes in the LEED patterns. No clear sequence of distances between the rows could be determined from STM images. Also, the high background in the LEED patterns does not allow one to distinguish two consecutive parallel stripes. More experiments are needed to compare this system with previous investigations by Ledieu *et al* on Cu thin films grown on *i*-Al–Pd–Mn [33, 34]. In this latter case, the atomic rows within the Cu domains were shown to follow a Fibonacci sequence. The main difference between the two systems is that Cu is deposited on the β phase and not directly on a fivefold QC plane as in the present case.

It is quite surprising, however, that the β phase is formed at room temperature on the *i*-Al–Cu–Fe but not on the *i*-Al–Pd–Mn. The fact that a new LEED pattern starts appearing already at 1 ML coverage suggests that there is already some intermixing taking place on the *i*-Al–Cu–Fe surface. The formation of the β phase is indeed expected on the basis of the large intermixing reported in Cu–Al bilayers (table 2). Also, intermixing was already mentioned by Barnes *et al* in a study of Cu/Al(111) system by LEED [35].

4.3. Annealing Cu/i-Al–Cu–Fe

For Cu thin film grown on Al, it is known that a critical thickness of the Cu film is needed to promote the formation of γ-Al_4Cu_9 [36, 37]. For the Cu/*i*-Al–Cu–Fe system also, the thickness of the Cu must be larger than some critical value in order to stabilize an interface region that will prevent fast diffusion of Cu into the bulk. In this way, the surface region may contain enough Cu to grow γ-Al_4Cu_9. To determine this critical value, we have annealed Cu films of different thicknesses on *i*-Al–Cu–Fe, namely $\theta = 5$, 8 and 20 ML.

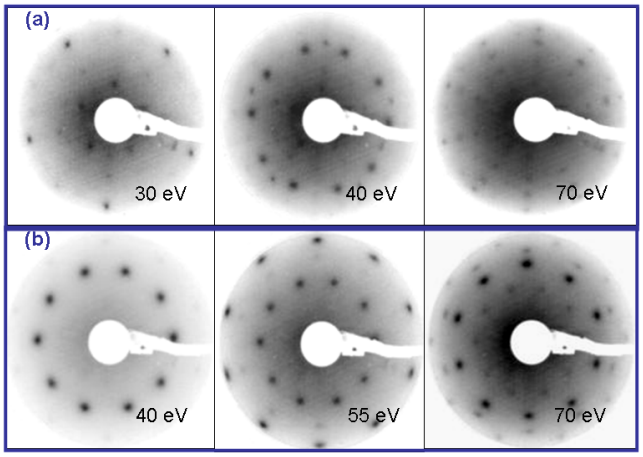

Figure 4. LEED patterns observed after annealing 5 ML (a) and 8 ML (b) of Cu/ *i*-Al–Cu–Fe at 573 K.

Figure 4 shows LEED patterns obtained during the annealing of 5 and 8 ML thick Cu films. The surface is annealed in front of the LEED optics and the heating power is switched off when a new pattern appears. For 5 ML annealed at 573 K (figure 4(a)), the LEED spots corresponding to the β phase become more intense and sharper. In addition, substrate spots reappear, indicating that there is either Cu desorption or diffusion into the bulk. For 8 ML annealed at 573 K, the pseudo-tenfold patterns correspond again to the β phase with (110) planes perpendicular to the fivefold axis of the substrate. The quality of the diffraction pattern is much better than those recorded after room temperature deposition, indicative of an improved structural order.

Figure 5 shows the LEED of the 20 ML thick Cu film annealed at 558 K. The complex pattern of figure 5(a) is interpreted as resulting from five domains of γ-Al_4Cu_9(110) rotated by 72° from each other. Indeed the experimental pattern can be reproduced by superimposing five reciprocal lattices of γ-Al_4Cu_9(110) rotated by 72° from each other (figure 5(b) and (c)). Similar results can be obtained by calculating the Fourier transform of five γ-(110) planes rotated by 72°, as shown in figure 5(d). The matching is almost perfect except for the outermost spots that do not belong to the γ phase. Those latter spots actually belong to some remaining β phase. Domains of γ-(110) appear in STM images as a set of parallel atomic rows separated by 12.31 Å (figure 6). Angles between atomic rows of adjacent domains are multiples of 72°. Measurements along atomic lines lead to a constant value of 8.8 Å, which is one of the two parameters of the γ-(110) unit mesh ($a = 8.71, b = 12.31$ Å). One can notice that other domains that do not present these atomic rows coexist with the γ phase (indicated by arrows in figure 6(b)). Those domains are attributed to the remaining β phase.

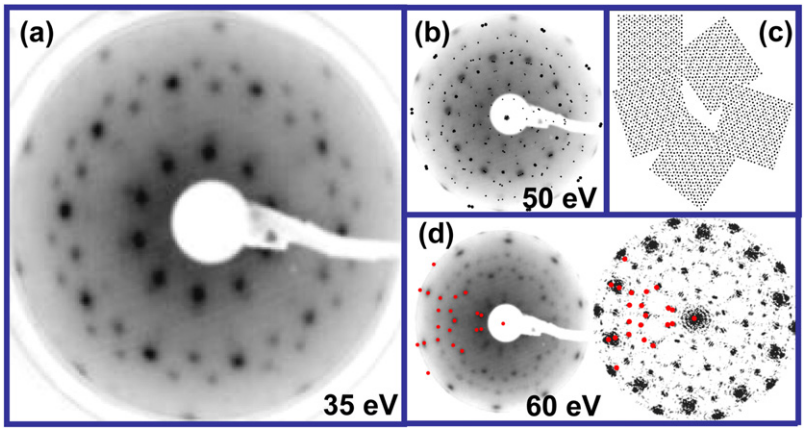

Figure 5. (a) LEED pattern for a 20 ML thick Cu film deposited on *i*-Al–Cu–Fe and annealed at 558 K. (b) and (c) show the good agreement obtained by matching the experimental LEED pattern (50 eV) with five calculated reciprocal lattices of γ-(110) domains rotated by 72°. (d) shows the correspondence between the experimental LEED pattern taken at 60 eV and the fast Fourier transform of five γ-(110) domains rotated by 72°.

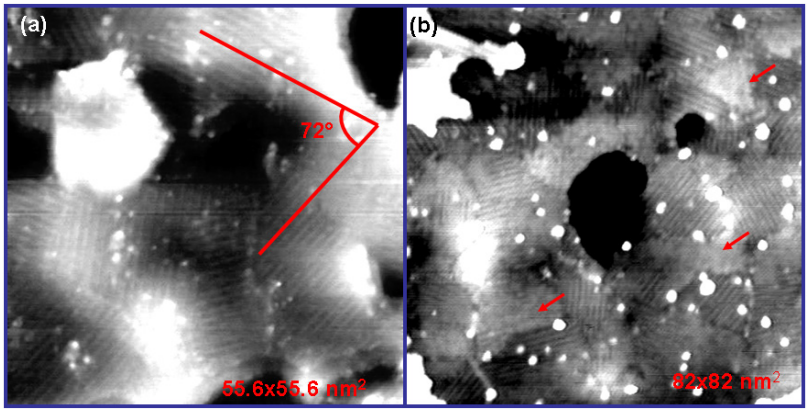

Figure 6. (a), (b) STM images of a 20 ML thick Cu film on *i*-Al–Cu–Fe and annealed at 558 K. Atomic rows are observed with γ-(110) domains. Some regions corresponding to untransformed β phase are indicated by arrows in (b).

4.4. Al/Al_4Cu_9/i-Al–Cu–Fe sandwich

We have seen that the γ-Al_4Cu_9 approximant can be grown easily on top of the QC, as long as the initial Cu film is thick enough. The interfacial relationship between the approximant and the QC substrate is defined by $[110]_\gamma \parallel$ 5f. We then grow a 10 ML thick Al film on the Al_4Cu_9/*i*-Al–Cu–Fe substrate. Figure 7 shows the corresponding LEED pattern recorded at 80 eV. It consists of two different sets of spots: a ring of 30 spots with a diameter corresponding to 2.80 Å in direct space together with a pseudo-tenfold pattern characteristic of the β phase. This is consistent with five domains of Al(111) rotated by 72° either on top or coexisting with the β phase. The β phase may be formed by destabilization of a part of the γ phase induced by Al diffusion at the interface. More insight could be provided by *in situ* STM measurements on such system.

This successfully demonstrates the possibility of growing a coherent buffer layer between a simple metal and a QC substrate. The interfacial relationships between the different layers are defined by Al(111)/Al_4Cu_9(110)/*i*-Al–Cu–Fe (5f).

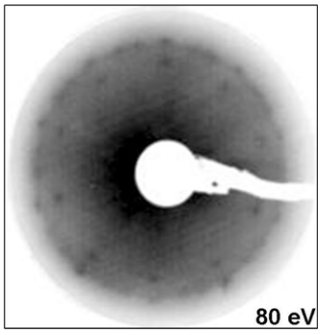

Figure 7. LEED pattern for a 10 ML thick Al film deposited on Al_4Cu_9/*i*-Al–Cu–Fe. The outer ring of 30 spots corresponds to a fivefold twinning of Al(111) with a lattice parameter of 2.80 Å whereas the inner ring of spots comes from β-(110) domains.

5. Summary

We have reviewed several examples where the formation of complex approximant phases on QC substrates was observed. These phases can appear either as a result of surface

phase transformations induced by preferential sputtering or evaporation of some component of the ternary alloy. They can also be formed in a controlled way by annealing a thin film deposited on the QC substrate. For Al-based QCs, the adsorbate element can be selected from among transition metals that form approximants when alloying with Al. To illustrate this approach, we have grown Cu films of different thickness on the fivefold surface of the *i*-Al–Cu–Fe QC. Low-temperature annealing of a 20 ML thick film is sufficient to promote the formation of the γ-Al_4Cu_9 approximant as a surface alloy. This phase is a Hume-Rothery alloy with physical properties intermediate between a simple metal and a QC, and could be used as an interface buffer layer to enhance adhesion between a QC coating and a metal substrate. Finally, we could form Al(111) domains on top of the fivefold twinning of γ-Al_4Cu_9(110) domains. The epitaxial relationships between the different layers of the complete stacking are defined by $[111]_{Al} \parallel [110]_{Al_4Cu_9} \parallel [5f]_{i\text{-Al–Cu–Fe}}$. We believe that this approach could be useful to tailor the adhesion of QC coatings on simple metal substrates.

Acknowledgment

We acknowledge the European Network of Excellence on Complex Metallic Alloys (CMA) contract NMP3-CT-2005-500145 for financial support.

References

[1] Park J Y, Ogletree D F, Salmeron M, Ribeiro R A, Canfield P C, Jenks C J and Thiel P A 2006 *Phil. Mag.* **86** 945
[2] Park J C and Thiel P A 2008 *J. Phys.: Condens. Matter* **20** 314012
[3] Balbyshev V N, Khramov A, King D J, Phillips B S, Kasten L S and Donley M S 2003 *Prog. Org. Coat.* **47** 357
[4] Dubois J M and Belin-Ferré E 2006 *Int. J. Mater. Res.* **97** 985
[5] Dubois J-M 2001 *J. Phys.: Condens. Matter* **13** 7753
[6] Boudard M 2000 *Quasicrystals: Current Topics* ed E Belin-Ferré, C Berger, M Quiquandon and A Sadoc (Singapore: World Scientific) p 73
[7] Dong C 1995 *Scr. Metall. Mater.* **33** 239
[8] Stadnik Z M 1999 *Physical Properties of Quasicrystals* (Berlin: Springer)
[9] Trambly de Laissardiere G, Nguyen-Manh D and Mayou D 2005 *Prog. Mater. Sci.* **50** 679
[10] Tamura N 1997 *Phil. Mag.* A **76** 337
[11] Ebert P, Feuerbacher M, Tamura N, Wollgarten M and Urban K 1996 *Phys. Rev. Lett.* **77** 3827
[12] Ledieu J, Diehl R D, Lograsso T A, Delaney D W, Papadopolos Z and Kasner G 2001 *Surf. Sci.* **492** L729
[13] Shen Z, Kramer M J, Jenks C J, Goldman A I, Lograsso T, Delaney D, Heinzig M, Raberg W and Thiel P A 1998 *Phys. Rev.* B **58** 9961
[14] Shi F, Shen Z, Delaney D W, Goldman A I, Jenks C J, Kramer M J, Lograsso T, Thiel P A and van Hove M A 1998 *Surf. Sci.* **411** 86
[15] Barrow J A, Fournée V, Ross A R, Thiel P A, Shimoda M and Tsai A P 2003 *Surf. Sci.* **539** 54
[16] Naumovic D 2004 *Prog. Surf. Sci.* **75** 205
[17] Naumovic D, Aebi P, Schlapbach L, Beeli C, Kunze K, Lograsso T A and Delaney D W 2001 *Phys. Rev. Lett.* **87** 195506
[18] Ledieu J, Muryn C A, Thornton G, Cappello G, Chevrier J, Diehl R D, Lograsso T A, Delaney D and McGrath R 2000 *Mater. Sci. Eng.* A **294–296** 871
[19] Fournée V *et al* 2002 *Phys. Rev.* B **66** 165423
[20] Woodruff D P 2002 *Surface Alloys and Alloy Surfaces* (Amsterdam: Elsevier)
[21] Gierer M *et al* 1998 *Phys. Rev.* B **57** 7628
[22] Sharma H R, Fournée V, Shimoda M, Ross A R, Lograsso T A, Tsai A P and Yamamoto A 2004 *Phys. Rev. Lett.* **93** 165502
[23] Cai T, Fournée V, Lograsso T A, Ross A R and Thiel P A 2002 *Phys. Rev.* B **65** 140202
[24] Zheng J C *et al* 2004 *Phys. Rev.* B **69** 134107
[25] Buchanan J D R, Hase T P A, Tanner B K, Chen P J, Gan L, Powell J C and Egelhoff W L 2002 *Phys. Rev.* B **66** 104427
[26] Shimoda M, Sato T J, Tsai A P and Guo J Q 2000 *Phys. Rev.* B **62** 11288
[27] Shimoda M, Guo J Q, Sato T J and Tsai A P 2001 *Surf. Sci.* **482–485** 784
[28] Weisskopf Y, Burkardt S, Erbudak M and Longchamp J N 2007 *Surf. Sci.* **601** 544
[29] Bielmann M, Barranco A, Ruffieux P, Gröning O, Fasel R, Widmer R and Gröning P 2005 *Adv. Eng. Mater.* **7** 392
[30] Dong C 1996 *Phil. Mag.* A **73** 1519
[31] Sharma H R, Shimoda M, Fournée V, Ross A R, Lograsso T A and Tsai A P 2005 *Appl. Surf. Sci.* **241** 256
[32] Villars P and Calvert L D 1998 *Pearson's Handbook of Crystallographic Data for Intermetallic Phases* (Materials Park, OH: ASM International)
[33] Ledieu J, Hoeft J T, Reid D E, Smerdon J A, Diehl R D, Lograsso T A, Ross A R and McGrath R 2004 *Phys. Rev. Lett.* **92** 135507
[34] Ledieu J, Hoeft J T, Reid D E, Smerdon J A, Diehl R D, Ferralis N, Lograsso T A, Ross A R and McGrath R 2005 *Phys. Rev.* B **72** 035420
[35] Barnes C J, Asonen H, Salokatve A and Pessa M 1987 *Surf. Sci.* **184** 163
[36] Jiang H G, Dai J Y, Tong H Y, Ding B Z, Song Q H and Hu Z Q 1993 *J. Appl. Phys.* **74** 6165
[37] Vandenberg J M and Hamm R A 1982 *Thin Solid Films* **97** 313